

CHARACTERISTICS OF A BETATRON CORE FOR EXTRACTION IN A PROTON-ION MEDICAL SYNCHROTRON

L. Badano¹ and S. Rossi^{1,2}

Abstract

Medical synchrotrons for radiation therapy require a very stable extraction of the beam over a period of about one second. The techniques for applying resonant extraction to achieve this long spill can be classified into two groups, those that move the resonance and those that move the beam. The latter has the great advantage of keeping all lattice functions, and hence the resonance conditions, constant. The present report examines the possibility of using a betatron core to accelerate the waiting ion beam by induction into the resonance. The working principle, the proposed characteristics and the expected performances of this device are discussed. The betatron core is a smooth high-inductance device compared to the small quadrupole lenses that are normally used to move the resonance and is therefore better suited to delivering a very smooth spill. The large stored energy in a betatron core compared to a small quadrupole is also a safety feature since it responds less quickly to transients that could send large beam spikes to the patient.

¹ TERA Foundation, via Puccini 11, 28100 Novara, Italy

² CERN, CH1211, Geneva 23, Switzerland

1. INTRODUCTION

A feasibility study of a dedicated medical synchrotron for accelerating protons and light ions (e.g. carbon) for cancer treatment is being pursued at CERN as a four-way collaboration between the TERA Foundation, AUSTRON, CERN and GSI. Medical synchrotrons require a long (about one second) and stable extracted beam current. One technique for achieving this quality spill is to accelerate an unbunched beam uniformly into a third-order resonance. Induction acceleration with a betatron core [i] (called simply a *betatron* from now on) is in use in Saclay [ii] (for similar applications) and Heidelberg [iii] (for other purposes than extraction) and has been recently proposed to drive the extraction process in a medical synchrotron [iv]. The use of a betatron in the extraction process is presented here and an evaluation of its main parameters is given with the aim of clarifying the smoothness of this device and the increased stability of the extracted spill intensity that represents an important advantage for medical synchrotrons. The first section will present the working principle of the betatron from which its technical characteristics will be deduced. The working cycle will then be studied to give the required current and voltage variations from the power supply. These characteristics will be the basis for the evaluation of the power supply requirements. An evaluation of the stability of this extraction technique and the influence of power supply ripple will also be presented.

2. THE WORKING PRINCIPLE

The proposed extraction method from the synchrotron is a third-integer resonant scheme driven by sextupoles.

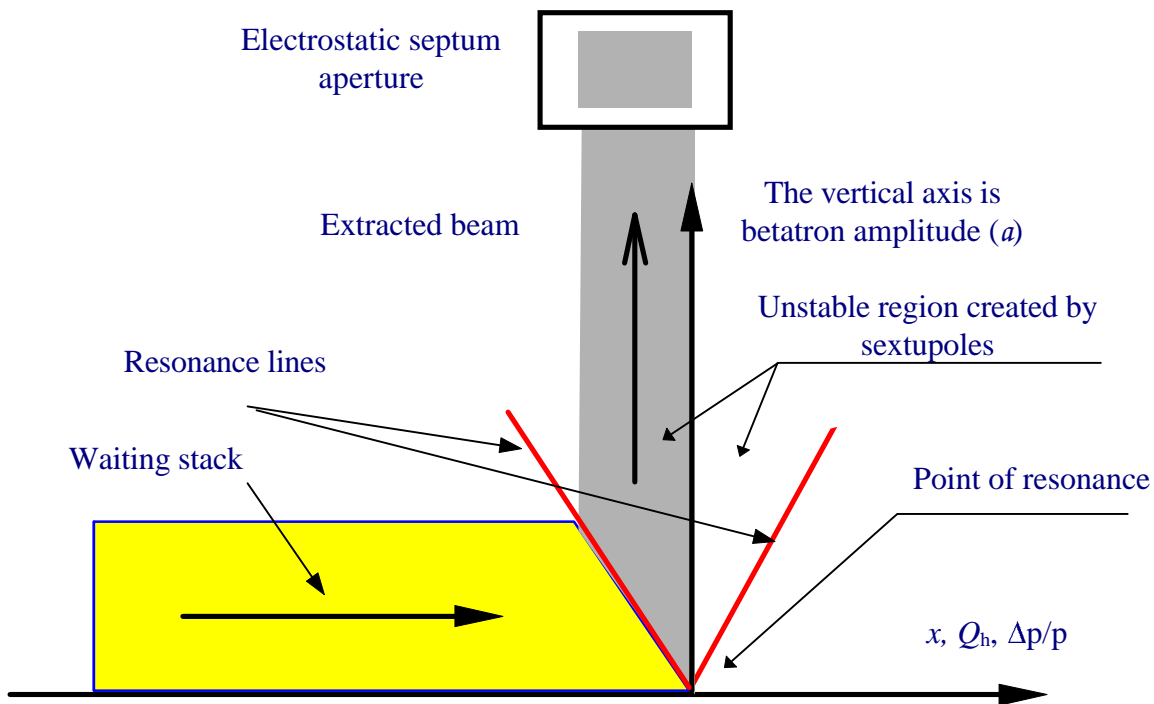


Fig. 1 The amplitude-tune diagram of the resonant extraction process.

The presence of one or more sextupoles in the synchrotron creates a region of instability in the phase space of the beam. Particles which have a betatron amplitude (a) are stable if:

$$a < 12 \sqrt{\frac{\pi}{\sqrt{3}}} \frac{|\Delta Q|}{|S_{sext}|} \quad (1)$$

where $\Delta Q = (\text{Particle tune} - \text{Resonance tune})$ and S_{sext} is the sextupole strength in normalised coordinates. These particles form the so-called “waiting stack” in Fig. 1. In the present proposal, at the end of the acceleration process, the beam is debunched and shaped with RF noise to acquire the uniform distribution shown in Fig. 1, but this is not a constraint since the betatron can be adapted to the extraction of beams with different distributions. Those particles that are in the unstable region increase their amplitude of oscillation during each turn until they enter the electrostatic septum aperture where they receive a kick and are deflected into the transfer line. The unstable region, defined by reversing the inequality in expression (1), is shown in Fig. 1 as the area between the resonance lines; the electrostatic septum is schematised on the vertical axis.

In the amplitude-tune diagram of Fig. 1, the horizontal axis is the position of the equilibrium orbit across the aperture of the vacuum chamber, x , but it can also represent the momentum spread, $\Delta p/p$, if the dispersion (D) is non zero, since $x = D \cdot \Delta p/p$, or the tune, Q_h , if the chromaticity (ξ_h) is non-zero, since $\Delta Q/Q_h = \xi_h \cdot \Delta p/p$. The purpose of the betatron, which is schematically presented in Fig. 2, is to smoothly accelerate the waiting stack into the resonance.

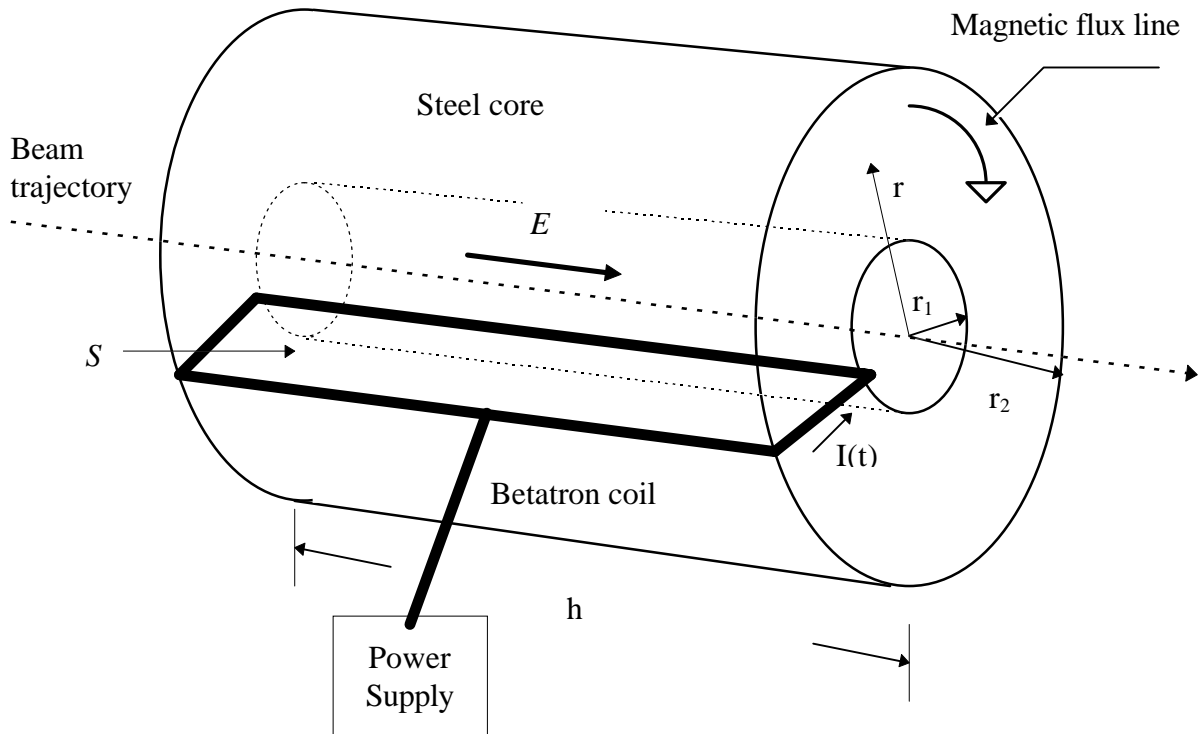


Fig. 2 Schematic view of the betatron.

The application of a time varying current $I(t)$ to the betatron coil excites a magnetic flux variation ($\Delta\phi$) inside the steel core. The flux variation with time produces an electrical field parallel to the axis of the betatron. If a particle of charge Ze passes along this axis, it experiences a variation of its kinetic energy E_c given by:

$$\delta E_c = Ze \frac{d\phi}{dt}. \quad (2)$$

The natural unit of time, during which the particle experiences the accelerating effect of the betatron, is the revolution period or the inverse of the revolution frequency f_r . Therefore, from (2), considering the relation between the momentum change of the particle and its kinetic energy variation, the necessary magnetic flux variation inside the iron core of the betatron required for a given momentum change (Δp) is expressed by:

$$\Delta\phi = (\gamma - 1) \left(1 + \frac{1}{\gamma} \right) \frac{m_0 c^2}{e} \frac{A}{Z} \frac{1}{f_r} \left(\frac{\Delta p}{p} \right) \quad (3)$$

where, A is the mass number, m_0 is the unit rest mass of a nucleon and γ the relativistic parameter.

In expression (3) only particle parameters appear. It is also useful, though redundant, to express the magnetic flux variation as a function of the synchrotron parameters. The Faraday-Neumann-Lenz law, relating the magnetic flux variation to the electric field that acts on a particle revolving on a closed orbit linking the betatron, states:

$$\oint \vec{E} \cdot d\vec{s} = - \frac{\partial}{\partial t} \iint \vec{B} \cdot d\vec{S} = - \frac{d\phi}{dt}. \quad (4)$$

Here the s coordinate describes the distance along the orbit. Introducing a mean value of the electric field (\bar{E}) over the machine circumference (C), and using the dynamic theorem:

$$\frac{dp}{dt} = Ze\bar{E} \quad dt = \frac{1}{f_r} \quad (5)$$

together with the Lorentz law that relates the momentum of the particle to its magnetic rigidity ($B\rho$):

$$p = -ZeB\rho \quad (6)$$

it gives from expression (4):

$$\Delta\phi = CB\rho \frac{\Delta p}{p}. \quad (7)$$

Both the expressions (3) and (7) can be used to calculate the total magnetic flux variation needed to produce the momentum variation required for the resonant extraction of the whole beam. To obtain a uniform sweeping of the beam through the resonance, the magnetic flux variation has to be constant in time, thus implying a constant voltage difference V_a across the betatron, “seen” by the beam during the extraction time (T_{ext}):

$$V_a = \frac{d\phi}{dt} = CB\rho \frac{\Delta p/p}{T_{ext}}. \quad (8)$$

3. ESTIMATE OF THE CORE CHARACTERISTICS

Table 1 summarises some basic parameters of the medical synchrotron that is being studied at CERN. The particles to be accelerated in the synchrotron are protons and light ions (i.e. fully stripped carbon ions), but in what follows only the light-ion extraction at the highest energy is examined, since this imposes the most stringent constraints on the betatron design.

Table 1 *Medical synchrotron design specifications.*

Circumference (C) [m]	75
Accelerated particles	$^{12}\text{C}^{6+}$
Charge to mass ratio (Z/A)	0.5
Number of circulating particles (N_p)	7.9×10^9
Extraction scheme	resonant (third-integer)
Maximum kinetic extraction energy (\hat{E}_c) [MeV/u]	400
$\beta = v/c$ at \hat{E}_c	0.715
$\gamma = 1/\sqrt{1-\beta^2}$ at \hat{E}_c	1.429
Momentum at \hat{E}_c [(MeV/u)/c]	951.417
Revolution period at \hat{E}_c [μs]	0.35
Beam intensity at \hat{E}_c [mA]	21.6
Magnetic rigidity at \hat{E}_c [T·m]	6.347
$\Delta p/p$ of the beam at \hat{E}_c [%]	0.4
Repetition rate [Hz]	1
Typical cycle	
injection and acceleration [ms]	200
flat top (extracted spill duration) [ms]	600 (500)
fall [ms]	200

The total momentum variation that will be used for the betatron specifications, is $\Delta p/p = 0.5\%$. It is assumed that the extraction process starts with a stack positioned at a $\Delta p/p = 0.1\%$ from the resonance and that the stack has up to $\Delta p/p = 0.4\%$. From expression (7), the total magnetic flux variation needed in the betatron to sweep the whole stack through the resonance is $\Delta\phi = 2.38$ Wb. The specifications of the betatron, are set keeping the parameters within feasible limits. The maximum value of the magnetic field in the betatron iron core, the maximum value of the current in the coil and the maximum value of the voltage delivered by the power supply are particularly critical. The characteristics of the betatron core are summarised in Table 2 with some references to Fig. 2.

Table 2 *Betatron core characteristics.*

Length (h) [m]	1.5
Internal radius (r_1) [m]	0.08
External radius (r_2) [m]	0.75
Area of a section perpendicular to the magnetic field lines (S) [m ²]	1.005
Lamination thickness [mm]	0.5
Steel density [kg/m ³]	7870
Steel mass (m_s) [kg]	2.062×10^4

The inner radius of the betatron is fixed by the dimensions of the vacuum chamber of the synchrotron taking into account the space needed for the windings of the coil (in the Blue-book [v], which reports the lattice design of a similar medical synchrotron, the physical aperture of the quadrupoles is 130 mm). The internal and external radii together with the length of the betatron determine the area of the section perpendicular to the magnetic field lines. This parameter is of fundamental importance since it allows the estimation of the average maximum value of the magnetic field in the iron core:

$$B_{\max} = \frac{\Delta\phi}{2S} \quad (9)$$

where S is the steel section. The factor 2 in the denominator of expression (9) is justified by the exploitation of the complete hysteresis cycle of the steel for the magnetic flux variation, thus reducing saturation in the iron core of the betatron. Since $\Delta\phi = 2.38$ Wb and $S = 1.005$ m², the average maximum value of the magnetic field in the iron core is $B_{\max} = 1.184$ T.

Expression (9) is used here to obtain a rough estimate of the maximum magnetic field in the betatron core and to choose the most suitable steel. In fact, the magnetic field, at a fixed value of the current in the coil, varies with the radial position inside the betatron core decreasing in magnitude for larger values of the radius. The range of B is large (between 0.88 T and 1.59 T at maximum extraction energy, as a function of r^{-1}) and the value of B_{\max} gives only an idea of the expected intensities. In the following calculation of the currents and voltages in the power supply, a detailed description of the material properties will be considered.

Many kinds of steel have been considered with similar properties [vi] and in this analysis the Cockerill steel used for the SPS (the CERN Super Proton Synchrotron) main magnets has been chosen. The reasons for this choice are mainly to minimise the required currents and voltages to run the betatron. In Table A1 of Appendix A, the characteristics of the proposed steel are summarised. No hysteresis effects are considered in the analysis presented.

Figs. 3a and 3b show the magnetisation curve of the steel, i.e. the dependence of the magnetic field versus the magnetic excitation and Fig. 4 shows the dependence of the relative permeability $\mu_r = \frac{B}{\mu_0 H}$ of the Cockerill steel versus the magnetic excitation.

From Fig. 3a it can be seen that the magnetic field reaches a relatively high value before saturation occurs (almost $B = 1.5$ T for $H = 600$ A/m). This corresponds, as shown in Fig. 4, to

high values of the relative permeability for low values of the magnetic excitation, lower than 600 A/m.

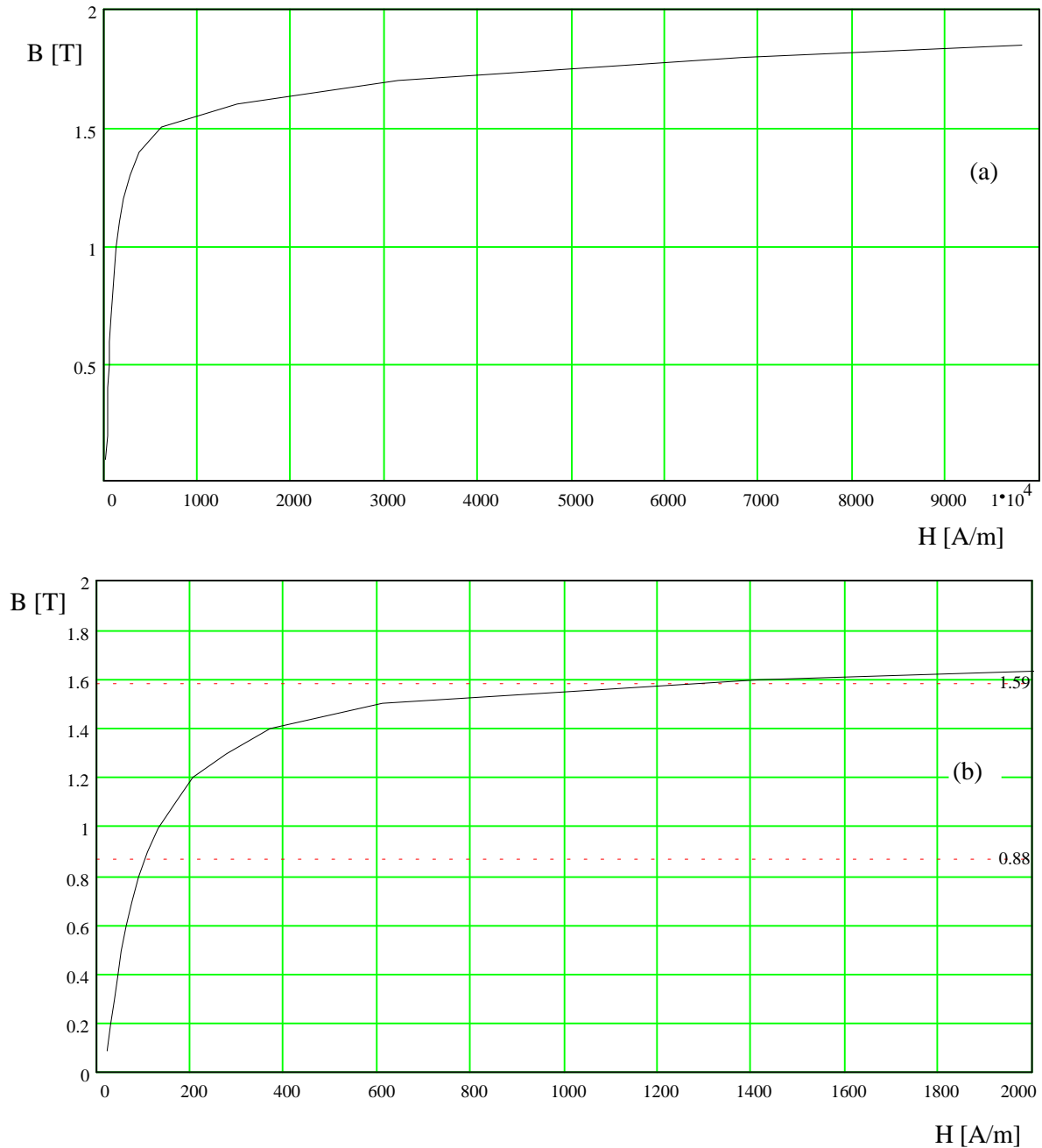


Fig. 3 Magnetisation curve for the Cockerill steel: (a) full representation; (b) detail of the first portion of the curve.

The fast rising start of the magnetisation curve is the most suitable region for the betatron working cycle, since, even if the inductance L is relatively high due to the large values of μ_r (see next section), the current variation with time, needed to obtain a constant magnetic flux variation, is small. When the magnetic field inside the betatron core increases above $B = 1$ T, the steel starts to saturate and a larger change of the current is needed for the same magnetic flux variation and, even if the inductance is decreasing, this results in a fast increase of the inductive component ($V_L = L(\mu_r) \frac{dI}{dt}$) of the voltage from the power supply.

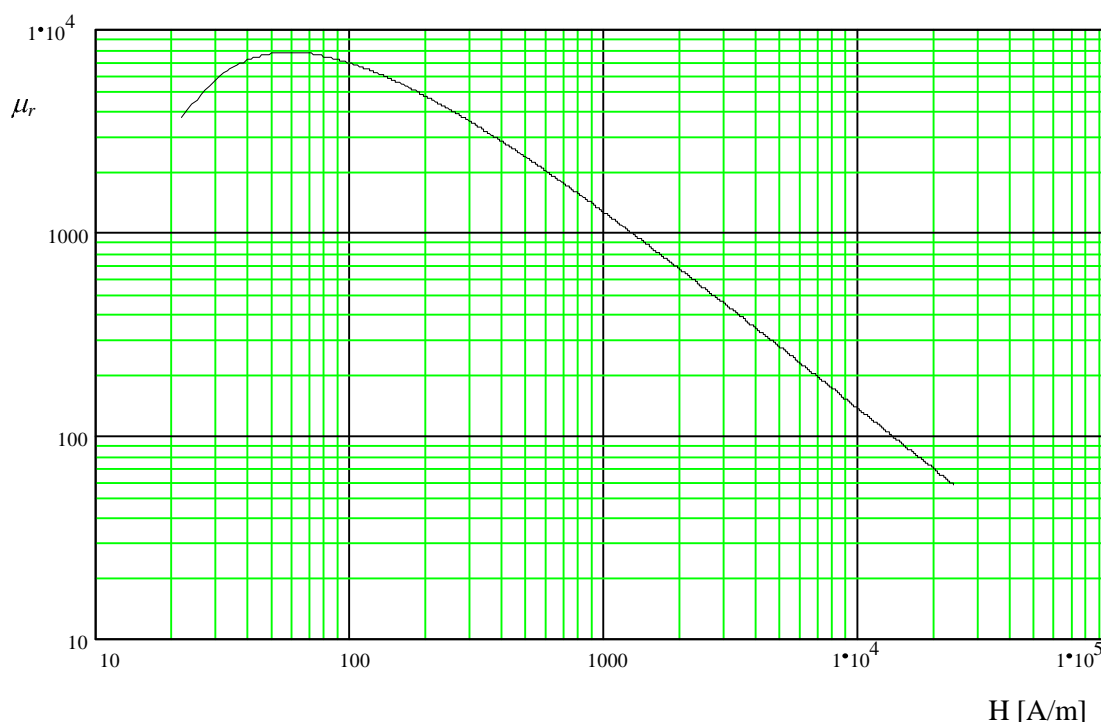


Fig. 4 Relative magnetic permeability of the Cockerill steel as a function of the magnetic excitation.

The lamination of the steel core can be done in the same way as for normal synchrotron magnets, i.e. laminating along the axis in the beam direction, but the large external diameter (1.5 m) will oblige the design to cut the betatron in two symmetric halves with respect to a plane containing the torus axis. Moreover, the large mass of the steel suggests that it would be better to divide the betatron core still further into units of shorter length to reduce problems of handling and installation.

4. ESTIMATE OF THE COIL AND OF THE POWER SUPPLY CHARACTERISTICS

4.1 The current cycle

As reported in Table 1, the cycle of the main magnets of the synchrotron (dipoles and quadrupoles) is divided into two parts: one for injection plus acceleration and fall (each one takes 200 ms), and one for extraction with a flat top duration of 600 ms. This slow extraction has been chosen to match the requirements of the active scanning system for delivering the dose to the patient. The spill duration (500 ms) allows the “painting” of a reasonable volume of the tumour, while keeping the treatment time, the active system specifications and the beam intensity within reasonable limits.

The current cycle in the betatron coil is represented in Figs. 5a and 5b. The requested current behaviour with reference to the points of maximum current amplitude, as shown in Fig. 5a, is not technologically feasible. For this reason, it is suggested that a small flat top of 80 ms is foreseen at the beginning and at the end of the extraction process. In addition, during the flat top before extraction it is possible to debunch and shape the beam as represented in Fig. 1. Thus, the reference current cycle is as shown in Fig. 5b.

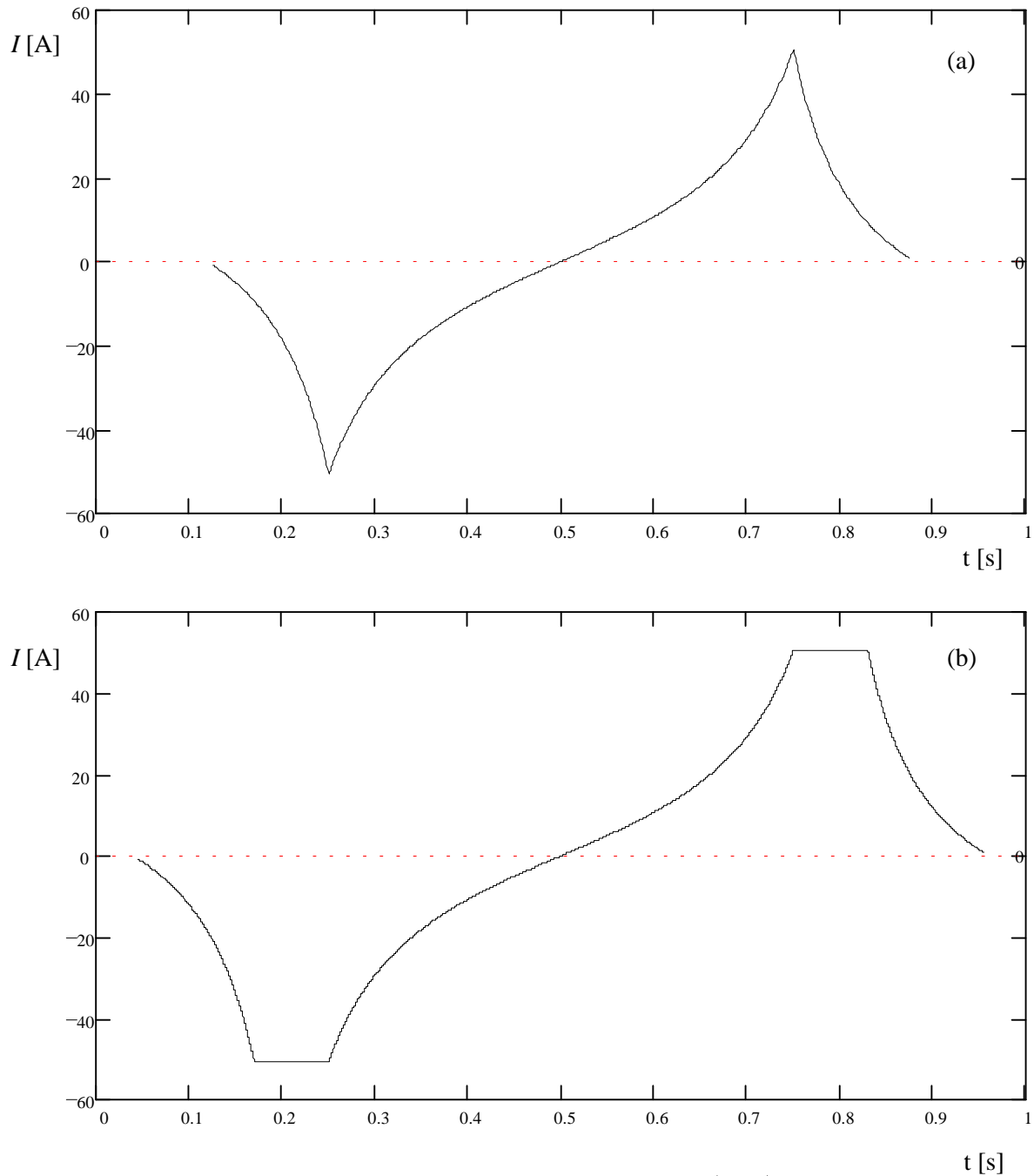


Fig. 5 The current I [A] versus time t [s] in the betatron coil, $|I_{\max}| = 51$ A: (a) basic cycle, (b) revised cycle (see the text for details).

During the first 45 ms of the main magnet cycle, no current is flowing in the betatron coil, since in this phase the injection and the capture of the beam is accomplished in the synchrotron and an active betatron could alter the injection and trapping efficiencies. Once the beam has been captured by the RF, the betatron is considered to give only a small perturbation to the beam dynamics.

Between 45 ms and 170 ms the current goes negative in order to bring the magnetic field in the steel core of the betatron to its maximum negative value. This value is fixed by the total

flux variation required during extraction and by the core dimensions, as previously mentioned. During this time interval, the RF provides the necessary restoring force to compensate the betatron effect. A time interval of 80 ms follows to allow the changing of the sign of dI/dt and to round the edges of the current profile (not shown in the figure). During this time interval there should be the debunching and the shaping of the beam. At $t = 250$ ms the extraction process starts and lasts till $t = 750$ ms. The current increases from its minimum value, corresponding to the minimum magnetic field, to its maximum value, corresponding to the maximum magnetic field, thus exploiting the whole rising part of the magnetic cycle of the core material. As already mentioned, in order to have an extracted beam of constant intensity (from a uniform rectangular beam shape, see Fig. 1) the magnetic flux variation has to be constant. The current behaviour represented in Fig. 5 satisfies this requirement taking into account the variation of the steel permeability with the magnetic excitation $H(I(t))$. At the end of the extraction process, the betatron returns to its standby position ready for a new injection. A time interval of 80 ms to change the sign of dI/dt is thus followed by an interval of 125 ms for the fall to zero.

As shown in Fig. 5, the current required from the power supply ranges between $I_{max} = \pm 51$ A. The current value depends inversely on the number of turns in the coil (N). In the present proposal the number of windings is set to $N = 10$. This choice is a compromise and it has been made by evaluating the maximum values of the current and inductance. In fact, while the current linearly decreases with N , the inductance quadratically increases with the number of turns thus giving larger values of the inductive component of the voltage. In the following section the variation of the inductance with N^2 and the dynamic change of the inductance due to the relative permeability of the steel will be examined.

4.2 The inductance of the betatron coil

The magnetic field inside the steel core is tangent to circles centred on the beam axis and its amplitude depends on the distance from the axis. For a radius $r_1 \leq r \leq r_2$ it is given by:

$$B(r) = \frac{\mu_0 \mu_r N I}{2\pi r} \quad (10)$$

where $\mu_0 = 4\pi \times 10^{-7}$ (Wb/m)/A is the magnetic permeability of the vacuum and I the current circulating in the coil. The integration of the magnetic field over the surface enclosed by a coil winding gives the magnetic flux per coil turn:

$$\phi = \int_{r_1}^{r_2} B(r) h dr = \frac{\mu_0 \mu_r N I}{2\pi} h \ln\left(\frac{r_2}{r_1}\right). \quad (11)$$

The total flux for the coil made of N windings is given by:

$$\phi = N\phi = \frac{\mu_0 \mu_r N^2 I}{2\pi} h \ln\left(\frac{r_2}{r_1}\right) \doteq LI. \quad (12)$$

From the last equality, that defines the inductance L of the coil, it follows that :

$$L(\mu_r) = \frac{\mu_0 \mu_r N^2}{2\pi} h \ln\left(\frac{r_2}{r_1}\right). \quad (13)$$

The steel properties and the dynamic behaviour of the excitation current enter into expression (13) through the relative permeability of the steel. As shown in Fig. 4, the relative permeability μ_r varies during the cycle and it implies a variation of the inductance of the coil as represented in Fig. 6.

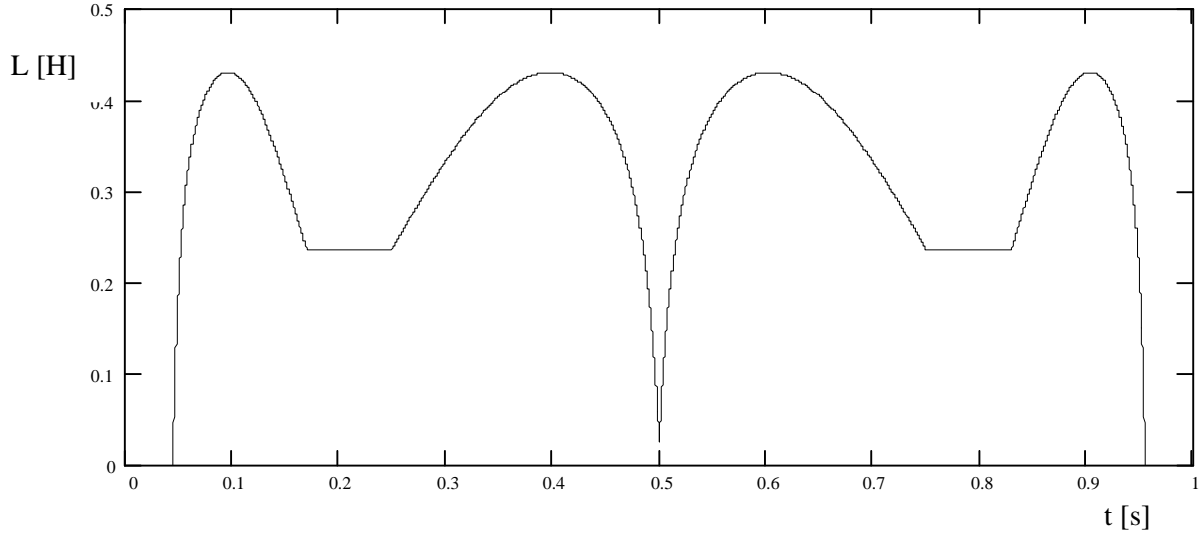


Fig. 6 Variation of the inductance with respect to time.

In spite of the reduced number of windings in the coil, the inductance is quite high during the betatron cycle. Although on one side this represents a drawback, since it increases the voltage required from the power supply, on the other side, it can be positively used to stabilise the voltage ripples of the power supply as will be discussed later. At the two extremes of the cycle, in Fig. 6, the reported value of the inductance is zero. This is an analytic extrapolation, since the inductance at these points is about 26 mH ($\mu_r = 300$). This simplification will be kept throughout the report without any significant error.

4.3 The resistance of the betatron coil and the dissipated power

To calculate the resistance and hence the dissipated resistive power of the betatron, the natural resistance of the copper windings (R_{cu}) has to be added to the equivalent resistance due to the eddy currents in the laminated steel core (R_{ec}) and to the equivalent resistance induced by the accelerated beam (R_b), since they act as energy dissipating components.

4.3.1 Losses due to the natural coil resistance

The previous section on current and inductance, together with the number of windings, makes it possible to fix the cross section (s_w) and the total length (l_w) of the copper wire of the coil: i.e. $s_w = 16 \text{ mm}^2$ and $l_w = 44 \text{ m}$. The cross section is chosen [vii] to avoid an overheating of the wire ($> 30 \text{ }^\circ\text{C}$) without water cooling. The maximum value of the current density is 3.2 A/mm^2 . The windings are insulated and their dimensions fit into the space between the core aperture

and the vacuum chamber. From the coil specifications (summarised in Table 3) it is possible to calculate the copper wire resistance:

$$R_{cu} = \rho_{60} \frac{l_w}{s_w} \quad (14)$$

where ρ_{60} is the copper resistivity at 60 °C. The copper resistance is equal to $R_{cu} = 0.055 \Omega$. The dissipated power during the whole cycle is $P_{cu} = 42.1 \text{ W}$.

4.3.2 Losses due to eddy currents

To compute the losses in a laminated steel core due to the eddy currents and to hysteresis, a classical estimate [viii] of the dissipated power for steel sheets of 0.5 mm of thickness is used:

$$P_{ec} [W] = P_0 \left[\frac{W}{kg} \right] \left(\frac{B_{max} [T]}{1[T]} \frac{f [Hz]}{50[Hz]} \right)^2 m_s [kg] \quad (15)$$

where $P_0 \cong 3.5 \text{ W/kg}$, $B_{max} [T]$ is the average peak magnetic field, $f [Hz]$ is the first harmonic of the magnetic field frequency (estimated to be 1 Hz in this case) and $m_s [kg]$ is the steel mass. The power consumption due to eddy currents in the laminated steel torus equals $P_{ec} = 47.7 \text{ W}$. This corresponds to an equivalent resistance $R_{ec} = 0.062 \Omega$.

4.3.3 Losses due to the beam current

During the extraction process, the betatron supplies energy (from the power supply) to the beam ($N_p = 7.9 \times 10^9$ is the number of circulating particles) in order to vary its momentum and to “push” it through the resonance. The kinetic energy gain of the beam corresponds to a dissipated power given by:

$$P_b = \frac{\Delta E_c}{T_{ext}} = \frac{1}{T_{ext}} \frac{1}{2} \left(1 + \frac{1}{\gamma} \right) \frac{\Delta p}{p} E_c N_p \quad (16)$$

that equals to $P_b = 0.05 \text{ W}$. The factor $\frac{1}{2}$ in the expression (16) accounts for a continuous extraction of a uniform beam. The equivalent resistance is $R_b = 1.2 \times 10^{-4} \Omega$.

4.3.4 Total resistance and total resistive power

The total load resistance, given by the sum of the described contributions, is $R_{tot} = 0.12 \Omega$ and the total resistive power is $P_{tot} = 89.8 \text{ W}$. It should be noticed that the resistive power required to operate the betatron is quite low, in spite of the large required values of the current and of the voltage. This behaviour is due to the high value of the inductance.

4.4 The required voltage rating of the power supply

From the current, the inductance and the total resistance so far calculated, it is possible to derive the resistive, V_R and inductive, V_L components of the total voltage V_{tot} to be delivered by the power supply. The two components and the total voltage, as a function of time, are shown in Fig. 7 and are given by the following expression:

$$V_{tot} = V_R + V_L = R_{tot}I + L(I)\frac{dI}{dt}. \quad (17)$$

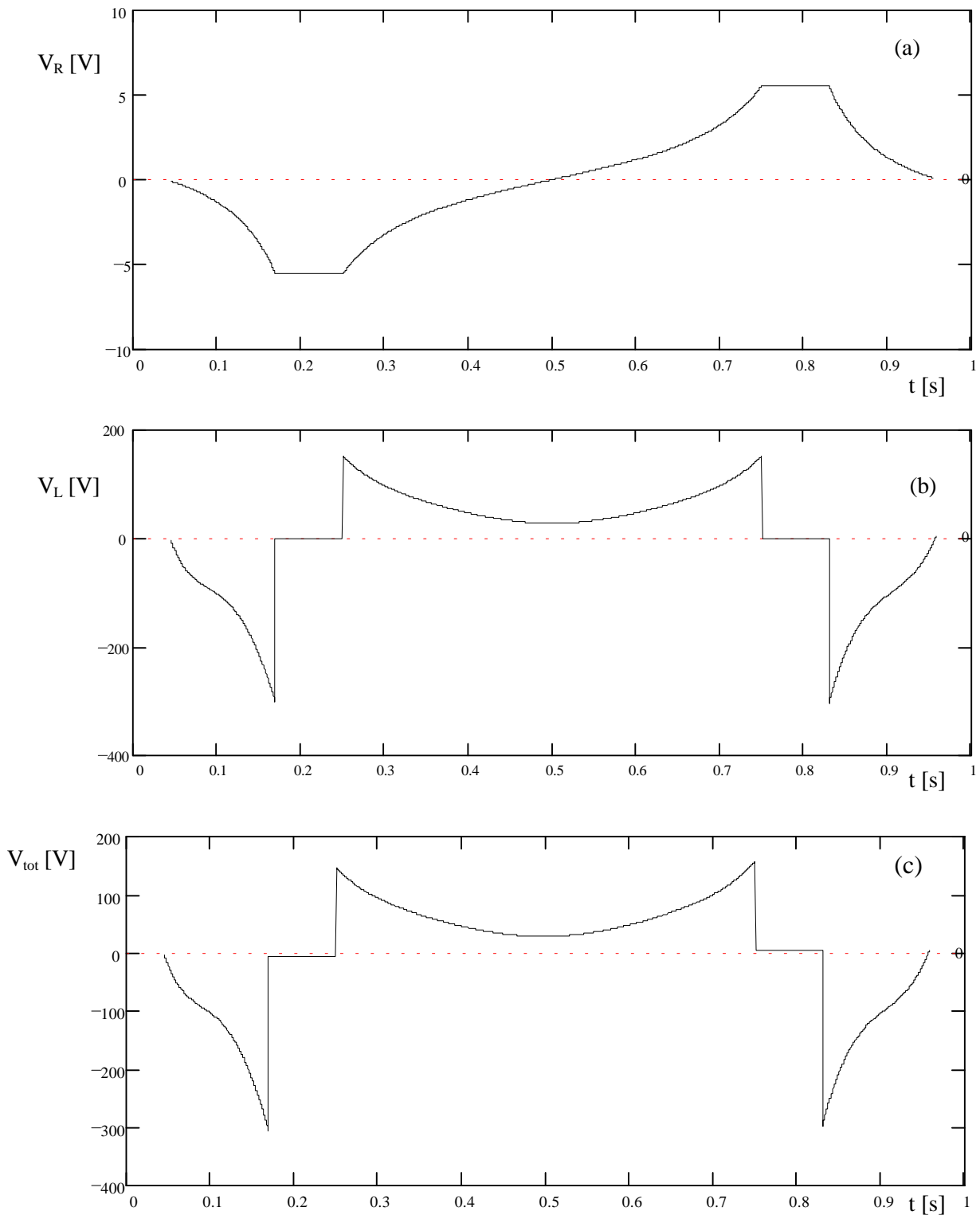


Fig. 7 Voltage versus time at the power supply output: (a) resistive component, (b) inductive component, (c) total voltage.

As shown in Fig. 7, the maximum absolute value of the voltage is $|V_{tot}^{max}| = 306$ V. The voltage behaviour is derived from the current cycle shown in Fig. 5b, but the extremes of the current flat-tops of 80 ms are rounded edges, so that the voltage change is smoother than what appears in Fig. 7. In addition, due to the high inductance load and its variation, a feed forward programming of the voltage must be foreseen. This will be useful at the beginning of the cycle in order to approach the minimum value of the voltage in a smoother way, thus better exploiting the initial low values of the inductance. Table 3 summarises the parameters of the betatron coil and the power supply. Due to the bi-polarity of both current and voltage, a four quadrant power supply is needed. In Appendix B a feasible scheme for the power supply is presented [ix]. The current is balanced between a series of two rectifiers and the current on the load is driven by varying the equilibrium point. A function generator allows the shaping of the current flow in the load as required in Fig. 5b.

Table 3 *Betatron coil and power supply [9] characteristics.*

Number of turns of the coil (N)	10
Section of the wire (s_w) [mm ²]	16
Length of the wire (l_w) [m]	44
Copper resistivity at 60 °C (ρ_{60}) [$\Omega \cdot m$]	2.035×10^{-8}
Maximum value of the inductance (L) [H]	0.43
Maximum absolute value of the current [A]	51
Maximum current density [A/mm ²]	3.2
Total coil resistance (R_{tot}) [Ω]	0.12
Total resistive power (P_{tot}) [W]	89.8
Maximum absolute value of the voltage [V]	306
Maximum current peak to peak variation [mA]	0.5
Current resolution	3.1×10^{-5}
Current reproduction accuracy	5.1×10^{-5}

The above specifications are the most conservative since they would extract the whole carbon beam at maximum energy in 250 ms (the time necessary to prepare the betatron for the extraction and to return to standby: 125 + 125 ms). It should also be underlined that, on a cycle to cycle basis, it is possible to adapt the betatron to different extraction energies and to different integrated extracted beam intensities (which, for example, could imply a different flux variation in the same time interval) in order to cope with the requests of an active beam spreading system for delivering the dose to the patient.

A betatron is currently used in Saclay to slowly extract particles from the synchrotron SATURNE II [ii]. The experience [x] showed that it took some time (a few weeks) to set the working parameters of the betatron power supply at the beginning of operations, but since this time they have been fixed and the system is remarkably stable and does not necessitate any particular maintenance.

5. EVALUATION OF THE BETATRON PERFORMANCES

In the first part of this section, an estimate is made of the momentum change induced by a current variation from the betatron power supply. The second part deals with the ripples and their influence on the B field. Furthermore, some considerations on DAC influence on spill quality are presented in Appendix C.

Consider the total relative momentum variation as the product of the current increase plus a small variation, with respect to the correct value, by a constant, so that the momentum variation can be considered as the sum of a nominal part and the contribution of the current variation:

$$\left(\frac{dp}{p}\right)_{bet} = cst \times (I + dI) = \left(\frac{dp}{p}\right)_{nom} + \left(\frac{dp}{p}\right)_{var}. \quad (18)$$

From the values in Table 3, the constant can be approximated by:

$$cst \approx \frac{1}{2} \left(\frac{\Delta p}{p}\right) / I_{max} = \frac{2.5 \times 10^{-3}}{51} = 5 \times 10^{-5} \quad (19)$$

so that, considering the absolute value of the current variation $dI = 0.5$ mA, it gives:

$$\left(\frac{dp}{p}\right)_{var} = 5 \times 10^{-5} dI = 5 \times 10^{-5} \times 5 \times 10^{-4} = 2.5 \times 10^{-8}. \quad (20)$$

To evaluate the effect of the power supply ripples let us consider a voltage, applied to the coil, of the form: $V_{coil} = V_0 + V \cos(\omega t)$. It generates a current $I = I_0 + I(\omega)$ such that the magnetic field is $B = B_0 + B(\omega)$ and, looking only to the frequency dependent term, it is possible to write:

$$I(\omega) = \frac{V}{\sqrt{R_{ec}^2 + (L \omega)^2}} \quad (21)$$

in which ω is the angular frequency of the ripple and as shown in expression (15), the equivalent resistance (R_{ec}) due to the eddy currents is increasing with the square of the frequency. This means that increasing the frequency and for a given voltage ripple the current ripple, and hence also the B field ripple which is proportional to $I(\omega)$, will decrease. Let us evaluate this current attenuation. With classical arguments [xi] it is possible to show that the equivalent resistance R_{ec} can be approximated by:

$$R_{ec} = k \frac{\sigma \omega^2 \mu_0 \mu_r}{8} L x^2 \quad (22)$$

where σ is the steel conductivity, L the inductance and x the lamination thickness of the betatron core; k is a correction constant that, for $\sigma = 10^7$ ($\Omega \text{ m}$)⁻¹, $\omega = 2 \pi \cdot 1$ Hz, $\mu_r = 4 \times 10^3$, $L = 0.24$ H, $x = 0.5$ mm, is equal to 4 to retrieve the value of $R_{ec} = 0.062$ Ω calculated from expression (15). Inserting the expression of R_{ec} in (21) it gives:

$$I(\omega) = \frac{V}{L \omega \cdot \sqrt{1 + \left(k \frac{\sigma \mu_0 \mu_r}{8} x^2\right)^2 \omega^2}} \quad (23)$$

from which it is possible to define a time constant for the eddy currents in the core given by:

$$\tau_{ec} = k \frac{\sigma \mu_0 \mu_r}{8} x^2. \quad (24)$$

From expression (23) a smoothing effect appears, due to the eddy currents, varying with the frequency. For a given voltage and increasing frequency, the current amplitude decreases by 20 dB/decade till the frequency reaches the critical value of $\omega_b = 1/\tau_{ec}$ when the slope starts to be 40 dB/decade. The current ripple (see expression (23)) is reduced by increasing the lamination thickness x ; in other words the pole frequency $\omega_b = 1/\tau_{ec}$ at which the slope of the attenuation becomes of 40 dB/decade becomes smaller. The present choice of laminations of 0.5 mm, which is commonly used in transformer designs, gives a time constant of about 6 ms. For example, for a voltage ripple of the order of 0.1 V at a frequency of 600 Hz, the resulting current ripple is of the order of 5×10^{-6} A, already a factor 100 smaller than the quoted low frequency value of about 0.5 mA. If necessary it is possible to further increase the eddy current time constant and the smoothing of the magnetic field ripples increasing the lamination thickness, but the power dissipation will increase.

6. FUTURE WORK

Work is underway and measurements have already been made on extracted spills using the betatron of Saturne II in Saclay [ii]. Fig. 8 shows for example an unoptimized extraction with a ripple of 2 kHz within about $\pm 20\%$ (corresponding to a duty factor of 0.98 [xii]).

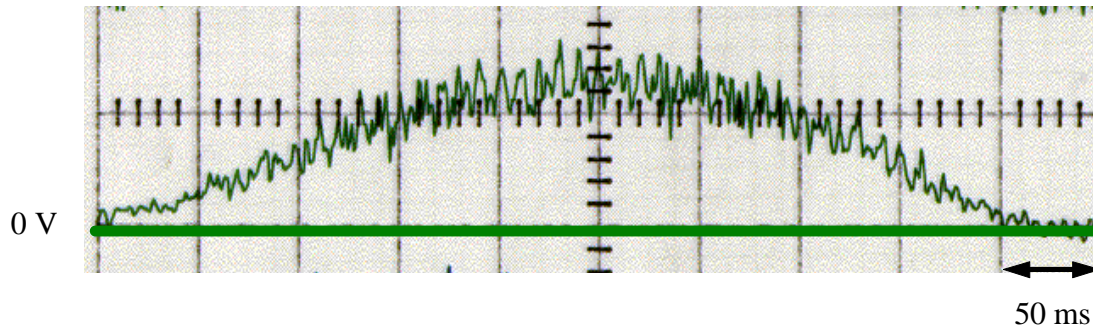


Fig. 8 Spill extracted with the betatron of Saturne II. Bandwidth of 2 kHz obtained integrating a measuring bandwidth up to 20 kHz.

This work is in its early stages and will be continued. In particular the possibility to introduce feed-back and feed-forward systems, acting on a single winding coil, to optimise the spill characteristics will be pursued. The use of the Vitrovac material to realise a more compact betatron core will also be investigated.

7. CONCLUSIONS

The use of a betatron to accelerate an unbunched beam into a third-order resonance to drive the slow extraction process has been studied. The working principle is relatively simple and the inductive force that “pushes” the beam into the resonance is largely independent of the beam characteristics thus giving a uniform acceleration. This last property is adapted to a beam that, at the end of the acceleration process and before extraction, has been debunched and

shaped with RF noise to acquire the uniform distribution shown in Fig. 1. It is nevertheless possible to adjust the betatron accelerating force to a more complex beam distribution generating a different function in the flux regulation system. In the present analysis, the starting point was the necessity to guarantee a constant variation of the magnetic flux with time. This requirement influenced both the choice of the material for the betatron core and the design features of the betatron coil. The proposed characteristics of the betatron components and also of the power supply are feasible. A better optimisation of the parameters is left to a later more detailed study. The specifications are the most stringent since they actually allow the extraction of the whole carbon beam at maximum energy in 250 ms. It has to be underlined that, on a cycle to cycle basis, it is possible to adapt the betatron to different extraction energies and to various integrated extracted intensities in order to cope with the requests of the active spreading system for delivering the dose to the patient.

By using a betatron core all lattice functions can be kept constant during extraction. This avoids the necessity of on-line orbit and focusing corrections that are features of the extraction systems that use quadrupoles to move the resonance. Since lattice elements have constant parameters, all lattice supplies are working under ideal conditions for the efficiency of their active filters, thus reducing to a minimum the ripple. The betatron power supply will be the only active element during extraction and particular care can be devoted to the optimisation of its performance. The lamination thickness can be optimised to increase the field ripple attenuation factor, but within the limits of a reasonable power dissipation.

ACKNOWLEDGEMENTS

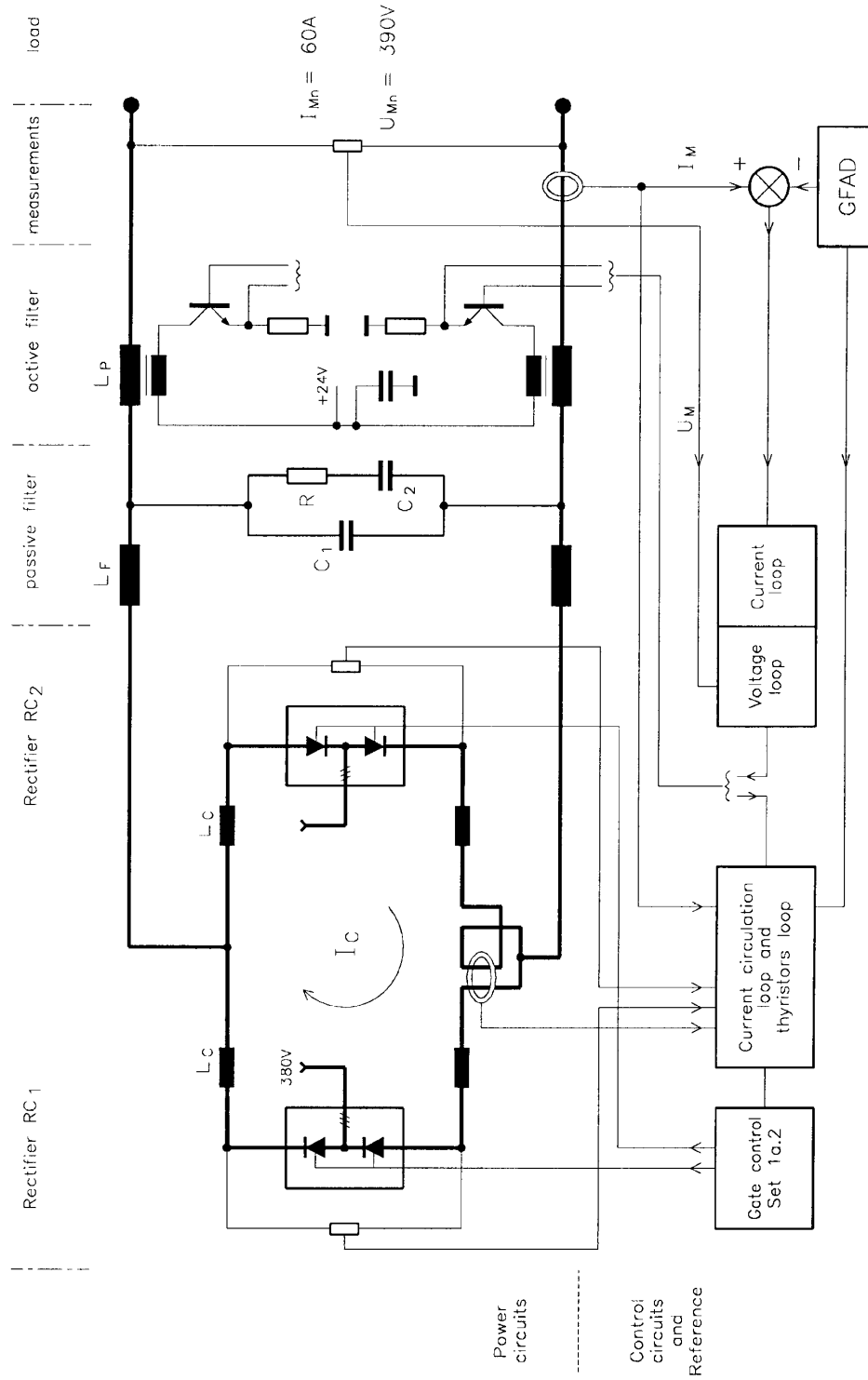
The authors are greatly indebted to J. Bosser (CERN) for his constant guidance throughout this work. We have also benefited from the advice given and discussions with J. Borburgh, P. Bryant, P. Burla, P.A. Chamouard (CEA - Saclay), M. Giesch, M. Gyr, J. Gruber (CERN), J.M. Lagniel (CEA - Saclay), R. Maccaferri, D. Möhl, O. Pagano, C. Steinbach, M. Thivent and M. Weiss (CERN). We also like to thank U. Amaldi (CERN and TERA Foundation) for the continuous support in the work, the PS Division for hosting this study and all the Saturne Group for their support and the possibility to perform tests on their machine.

APPENDIX A

Table A1 *Magnetic excitation, magnet field and relative permeability of the Cockerill steel [vi].*

H [A/m]	B [T]	μ_r
0	0	300
22.1049	0.1	3600
28.4205	0.2	5600
35.8996	0.3	6650
43.6041	0.4	7300
51.6737	0.5	7700
62.0084	0.6	7700
73.7804	0.7	7550
89.0377	0.8	7150
107.699	0.9	6650
131.533	1.0	6050
166.734	1.1	5250
207.593	1.2	4600
275.869	1.3	3750
371.362	1.4	3000
612.134	1.5	1950
1414.71	1.6	900
3146.09	1.7	430
6820.93	1.8	210
9814.55	1.85	150
15915.5	2.0	100
23873.2	2.1	70

Appendix B: The current source for the betatron



Appendix C: Consideration on DAC influence on spill quality.

Problem:

Using a 16-bit unipolar DAC, a *resolution* of 1 bit corresponds to a relative current change, in average, expressed by:

$$\frac{\Delta I}{I_{full\ scale}} = \frac{1}{2^{16}} = 1.5 \times 10^{-5}$$

The *accuracy* is better than $\pm \frac{1}{2}$ bit around the theoretical value: a change of the digital number by 1 bit corresponds to a change in the actual voltage of $(1 \pm 0.5) \cdot V_{bit}$. At full scale over one second this relative error appears at a frequency of about 66 kHz. But if we consider different vectors with different slopes to be given by the function generator, the frequency at which this error appears are varying and possibly as low as 1 kHz. In addition, the range used on the DAC will change when particles at different energies are extracted. This means that the relative error will increase accordingly. For example, if 20% of the power supply range is needed to extract particles over 1 second then a 16-bit DAC will give steps with a resolution of 8×10^{-5} at an average of 13 kHz. This should be compared to the sampling frequency for dosimetry of 10 kHz and to the power supply ripple requirements.

Considerations:

The phenomenon just described exists for all the power supplies driven by digital function generators (all the magnets and RF power supplies of the machine). *If during extraction all the power supplies except one (the betatron) are in steady state conditions, then all the problems are reported to that single power supply which should be constructed in a more careful way.*

(i) Higher precision DAC

When considering different extraction energies and different particles to be accelerated, it is possible to change the power supply range so as to work with a DAC which has its maximum amplitude as near as possible to the desired full scale. In such a case the current resolution and the modulating frequencies remain about the same. The drawback is that the gain cannot be changed on a cycle to cycle basis (it requires a few minutes to check precision), but it is suited if the use of protons and carbon ions is not continuously interchanged. However, this is only a partial solution since in practice it is usual to have many vectors in the function generator and many modulating frequencies may also be in the region of 1 - 10 kHz.

(ii) LHC technology

The 16-bit DAC, used as an example above, is already considered to be the practical limit with commercially available technology, although some 18-bit DACs do exist. A scheme for reaching 20 bit precision by reading back the current through a 20-bit ADC is being developed for the CERN LHC, but this requires long integration times to stabilise. It would have to be clarified whether this technique could be made to work for the relatively fast ramping needed in a medical synchrotron. Assuming that a 20 bit precision is possible:

$$\frac{\Delta I}{I_{full\ scale}} = \frac{1}{2^{20}} = 10^{-6}$$

then the uncontrolled ripple (about $\delta I \approx 0.5$ mA in the proposed conventional four quadrant power supply for the betatron) must be reduced since then the current resolution is about:

$$\frac{100\ A\ (full\ scale)}{2^{20}} \cong 0.1\ mA$$

thus implying a more careful control of the stability of the system. With a 20 bit precision the unit voltage step is:

$$\frac{10\ V\ (full\ scale)}{2^{20}} \cong 10\ \mu V$$

where 10 V is the typical full scale of the DAC. This step has to be compared, for example, with the temperature stability of the system: $10\ \mu V/^\circ C$ which is of the same order of magnitude.

(iii) Smoothing the DAC

Another approach is to filter the DAC output. The DAC step amplitude is actually filtered by the DAC itself (a reasonable rise time for the pulse is about 5 times smaller than the inverse of the DAC frequency) thus already reducing the actual bit amplitude and approaching a smoother rising curve. In addition it is possible to reduce drastically the discontinuity of the DAC step applying a vector generator method [xiii] that anticipates and smoothes out the DAC discontinuity. With this method, a reduction of the DAC error of at least a factor 100 is possible. Still in the case of a unipolar 16-bit DAC it means that a relative error of:

$$\frac{\Delta I}{I_{full\ scale}} \approx 10^{-7}$$

is achievable. This value seems quite acceptable. It should be noted that such small values approach the limit of measurement.

REFERENCES

- [i] K. Johnsen, Betatron core for the electron storage ring, PS/Int. AR/60-29.
F.A. Ferger, The design of the betatron core for the 2 MeV storage ring, AR/Int. SR/62-14.
- [ii] J.C. Ciret, Extraction du faisceau de Saturne II par acceleration betatronique. Le Gephyrotron, GERMA 76.02/IE-117 (1976).
- [iii] Ch. Ellert, D. Habs, E. Jaeschke, T. Kambara, M. Music, D. Schwalm, P. Sigray and A. Wolf, An induction accelerator for the Heidelberg Test Storage Ring TSR, Nucl. Instr. And Meth. A314 (1992) 399-408.
- [iv] Ch. Steinbach, Betatron Acceleration during Extraction, Minutes of the Meeting on Slow Extraction from Synchrotrons for Cancer Therapy, CERN 13-14 February 1996.
- [v] U. Amaldi and M. Silari editors, The TERA Project and the Centre for Oncological Hadrontherapy, INFN-LNF, Frascati, 1995, 2nd Ed., Vol. II, p. 302.
- [vi] M. Gyr and M. Giesch, private communications.
- [vii] Techniques de l'ingénieur, Paris, Electronique Edition (1953).
- [viii] K. Gieck, Formulaire technique, Ed. Giek-Verlag, D-7100, Heilbronn (1986).
- [ix] J. Gruber, private communication.
- [x] J.M. Lagniel, private communication.
- [xi] M. Rouault, Électricité, Ed. Masson & C, Paris, 1965, Vol. I, p. 158.
- [xii] P.J. Bryant, Spill quality and duty factor, Minutes of the Meeting on Slow Extraction from Synchrotrons for Cancer Therapy, CERN 2-3 September 1996.
- [xiii] J. Bossler, Rappel sur les systemes lineaires echantillonnes, SPS/ABM/Note/84-10.